An atom-transparent photon block for metal-atom deposition from high-temperature ovens

Richard Murdey, S. J. S. Liang, and J. Todd Stuckless

Citation: Review of Scientific Instruments **76**, 023911 (2005); doi: 10.1063/1.1855315
View online: http://dx.doi.org/10.1063/1.1855315
View Table of Contents: http://scitation.aip.org/content/aip/journal/rsi/76/2?ver=pdfcov
Published by the AIP Publishing

An atom-transparent photon block for metal-atom deposition from high-temperature ovens

Richard Murdey, S. J. S. Liang, and J. Todd Stuckless[a)]
Department of Chemistry, University of British Columbia, 2036 Main Mall, Vancouver, British Columbia, Canada V6T 1Z1

(Received 19 January 2004; accepted 12 October 2004; published online 25 January 2005)

We describe, in the context of polymer metallization calorimetry, the design and operation of a dual-chopper velocity selector to filter out the radiation background from high-temperature metal-atom oven sources. Particular attention is given to the resultant nonuniform atom flux profile. © *2005 American Institute of Physics.* [DOI: 10.1063/1.1855315]

I. INTRODUCTION

The physical vapor deposition of metals is a fundamental procedure in materials science, and a variety of techniques have been employed to generate metal-atom beams. Often, the source metal undergoes direct excitation by electron, ion, or laser bombardment, especially when the metal is refractory and when high atom fluxes are required. However, in many cases, it is preferable to achieve an equilibrium effusion of the atoms from a heated oven. An effusive source can deliver a very clean beam, relatively free of dimers, clusters, and ions, and the atoms have a well-characterized thermal distribution of velocities with a relatively low average kinetic energy. In order to increase the flux, ovens are often constructed with an orifice which is larger than the mean-free path (MFP) of the metal vapor atoms, and while this creates pressure gradients which alter the beam characteristics somewhat, these "pseudoeffusion" sources still provide a clean stable low-energy beam.[1,2] The primary limitation of such a source is that most metals have very little volatility, and so the effusion cell has to operate at extremely high temperatures. However, ovens constructed from suitable refractory materials, and with good differential pumping between source and target, are quite useful for depositing main group elements, noble metals, alkali and alkali earth metals, and a few transition metals.

An issue with high-temperature metal-atom sources, which we address here, is the thermal radiation load that they create at the deposition substrate. For many applications this is not important, however it can be a problem if the sample is photosensitive, or if it is poorly connected to its heat sink and suffers a large temperature rise, or if one is trying to perform optical measurements which are frustrated by scattered light. The radiation load at a given atom flux can be minimized by placing the oven further from the sample and operating it at a higher temperature, since the atom flux increases exponentially with temperature (in the molecular flow regime) while the thermal radiation only increases as $\sim T^4$. However, a hotter oven assembly produces more outgassing, and also in our experience the beams are less stable.

Oven radiation has an especially direct effect on attempts to calorimetrically measure the heat of reaction of metal atoms as they are deposited. In these experiments, the thermal sensor used to measure the reaction heat is also heated by oven radiation, and the two components must be separated. The information so obtained provides insight on the chemical bonds affecting interfacial adhesion, corrosion resistance, and the optical and electronic properties of deposited metal films. The metallization calorimetry technique was initially developed by Campbell *et al.*,[3–6] and we have recently furthered it to polymer metallization studies, with application especially to microelectronics and molecular electronics.[7,8]

In order to obtain sufficient flux, our sources are typically operated with a high enough vapor pressure that the MFP of the atoms is smaller than the size of the orifice diameter, at which point the effusion is attenuated by intermolecular collisions and the source becomes less efficient. As an example, we will discuss here a copper atom source with a 7 mm diameter orifice, operated at 1300 °C. This pseudoeffusion cell should provide an angle integrated fluence which is less than the 8×10^{17} atoms/s calculated[1] assuming true effusion, and so even with a large reaction heat of 300 kJ/mol would generate under 0.4 W of "chemical" energy. By comparison, given an emissivity of 0.15 for the molten copper,[9] the power of the radiant thermal energy is $\sim$2 W. This bright white light is emitted from the oven in an angular distribution similar to that of the atoms and, depending on the source design, there will also be scattered light from other regions of the oven assembly as tens of watts of power are dissipated in the heating elements. The actual radiation load on the sample depends also on the reflectivity of the sample. In our calorimetry experiments with this copper atom source, we typically measure a radiation heat signal that is approximately 500% the chemical heat signal. We expect the ratio of radiant to chemical heat to lie between 300% and 1000% for a variety of systems of interest, including depositions of Ag, Al, Cr, and Pd.

If the radiation load is not too much larger than the chemical heat generated, and is stable, it can be subtracted out as background from the total heat signal measured. One can estimate this background value using an extrapolation of

a)Electronic mail: johntodd@chem.ubc.ca

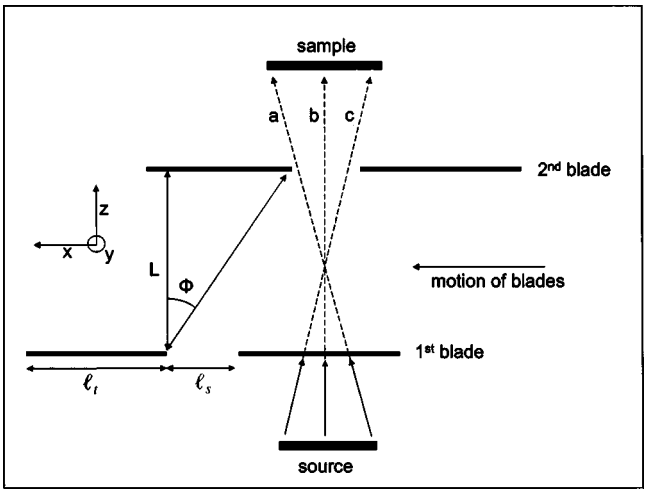

FIG. 1. Schematic of the velocity selector geometry, showing the slot width ℓ_s, the tooth width ℓ_t, and the pitch angle ϕ. Some example atom trajectories are shown, labelled *a*, *b*, and *c*. Trajectories are continuously being initiated from the oven, but will only pass unblocked within a time window dependant on the geometry and blade velocity.

the radiation signal measured at lower temperatures where the atom flux is negligible, however for accuracy this extrapolation would require knowing the thermal emission spectrum of the source and the reflectance spectrum of the sample. A more certain technique[3] is to measure the background signal when a window is translated into the atom beam, blocking the metal but letting most of the radiation through. However, this can be problematic if the reflectance of the sample changes substantially during the deposition, since frequent measurements of the radiation load are then required, and the accumulation of metal on the blocking window lowers its transmission. This is especially relevant to polymer metallization experiments where, for example, we find that the radiation absorbed from a 1300 °C oven increases by ~40% over a deposition range of only a dozen atomic layers of copper on a thin polyimide film on a gold-coated substrate.

We present here an alternative means of dealing with the radiation, which is to filter the photons out of a chopped atom-beam by using a second chopper as a "velocity selector" on each pulse. The opening of the two chopper blades is staggered such that there is never a direct line of sight open between the source and sample, so the photons are always blocked. However, the slot on the second blade opens quickly enough after the first blade has closed that the slower atoms, when they do arrive, pass through unblocked. Since the atoms from a high temperature source will have velocities on the order of tens of thousands of centimeters per second, and the sample needs to be within tens of centimeters from the oven to obtain high flux, the velocity selector needs to turn very quickly to have good transmission characteristics. A detailed analysis follows.

II. ANALYSIS OF ATOM TRANSMISSION CHARACTERISTICS

Figure 1 is a schematic (not to scale) of the beam and chopper assembly, showing some of the possible atom trajectories between the source and sample. Slow atoms have their best chance of reaching the sample when their trajectory intercepts the first blade soon after it has opened, as this allows more time to reach the second blade before it closes. Conversely, fast atoms have their best chance when they pass the first blade just before it closes, so there is less wait for the second blade to open. This last consideration is the most critical, as it will be difficult to spin the chopper fast enough to open the second blade before most of the atoms have already struck. We note that the teeth on the first and second chopper blades must overlap sufficiently to block all photon trajectories to the sample, and to allow for some tolerance in mounting of the assembly.

Our analysis of the transmission follows a reading of van den Meijdenberg.[10] First, we consider only nondivergent atom trajectories, i.e., normal to the planes in which the chopper blades lie. In the limit of the slot on each blade being infinitesimally narrow, and offset from each other by a pitch angle ϕ, then the only atoms which pass are those with velocity $v_0=\omega/\phi L$, where ω is the angular velocity of the blades and L is the distance between them (the thickness of the blades is assumed negligible compared to L). The slots on the first and second blades actually have arc lengths ℓ_{sa} and ℓ_{sb}, with the arc length between their leading edges given by $r\phi$ where r is the distance of the slots from the axis of rotation of the choppers (we assume that the slot depth is much smaller than r). The arc length described by motion of the slots while an atom of velocity v transits between the blades is equal to $r\omega L/v$. So, if we consider atoms with velocity less than v_0, the rotational arc length over which atoms are transmitted through the *pair* of blades is given by $\ell_{sb}-(r\omega L/v-r\phi)$ or by ℓ_{sa}, whichever is shorter. Similarly, if we consider atoms with velocity greater than v_0, then the open arc length is either $\ell_{sa}-(r\phi-r\omega L/v)$ or ℓ_{sb}, whichever is shorter. Neglecting asymmetry in the atom velocity distribution, and given that no line of sight is allowed through the two blades, it follows that the highest total throughput occurs where $\ell_{sb}=\ell_{sa}$.

The rotational arc length over which atoms of a given velocity are transmitted through the pair of blades can be considered as an "effective" slot width. The velocity dependent transmission probability of the assembly is simply the duty factor defined by this effective slot width. In consideration of the foregoing we write the transmission probability function, $B(v)$:

$$B(v)=\frac{\eta}{\gamma}\left(\gamma+1-\frac{L\omega}{\phi v}\right) \text{ for } v_{\min}\leqslant v\leqslant\frac{L\omega}{\phi}$$

$$B(v)=\frac{\eta}{\gamma}\left(\gamma-1+\frac{L\omega}{\phi v}\right) \text{ for } \frac{L\omega}{\phi}\leqslant v\leqslant v_{\max} \quad (1)$$

where $\gamma=\ell_s/r\phi$ is the ratio of the slot width to the slot offset, and η is the duty factor of the identical *individual* blades. The minimum and maximum atom velocities that can be transmitted are given by $v_{\min}=L\omega/(1+\gamma)\phi$ and $v_{\max}=L\omega/(1-\gamma)\phi$.

Next, we consider divergence of the beam, those atom trajectories which are not normal to the planes the blades lie

in. The velocity components tangential and radial to the motion of the blade as it intercepts the trajectory have a very different significance. We will assume that the radius of the choppers, r, is much larger than that of the beam, so that the arc of travel across the beam is almost linear, and label the tangential and radial directions as the x and y axis, respectively. Divergence in the y direction only effects transmission to the extent that the path length between the blades depends on that angle. Divergence in the x direction is more critical because a slot will reach different positions along the x axis at different times. This effect can be calculated by transforming the pitch angle in Eq. (1) to

$$\phi'(x_1,x_2) = \phi + \frac{L}{r}\alpha(x_1,x_2), \tag{2}$$

where α is the angle of divergence in the x-z plane defined by points at the source with $x=x_1$ and points at the sample with $x=x_2$. For each point on the sample, we integrate the flux from all points on the source, in each case using a transmission function $B'(v,x_1,x_2)$ that is calculated using ϕ'.

The transmission calculation involves an integration over the velocity distribution of the atoms as they arrive at the choppers. We will consider a nonequilibrium oven source later. For an equilibrium oven source, the number of atoms with velocity between v and $v+dv$ is given by the product of the Maxwell–Boltzmann distribution function and the total atom density, n. Then, the flux of atoms of a given velocity through the orifice is weighted by the component of the velocity normal to the orifice plane, $v\cos(\theta)$. So the flux per unit solid angle emitted in the direction θ is given by integrating the function:[11]

$$g(v)dv = n\left(\frac{M}{2\pi RT}\right)^{3/2}\exp\left[\frac{-Mv^2}{2RT}\right]v^3\cos(\theta)dv. \tag{3}$$

The flux per unit area which this generates at the sample is inversely proportional to the square of the distance from the source point to the sample point. Typically, the separation between the source and sample is much larger than their diameters, so this distance is approximately equivalent for all trajectories. In this limit, we can also ignore the effect of divergence in the y-z plane on transmission through the velocity selector. Integrating over all points on the source, the number of atoms arriving at any point on the sample is then determined by:

$$T(x_2,y_2) = \int_{y_1}\int_{x_1}\int_{v}\frac{g(v)}{d^2}B'(v,x_1,x_2)dvdx_1dy_1. \tag{4}$$

III. VELOCITY SELECTOR DESIGN

It is apparent early in the design process that very high rotational speeds are required for the velocity selector choppers, on the order of 10 000 rpm or higher. Conventional ultrahigh vacuum (UHV) rotary feedthroughs, which use either a bellows seal or magnetic coupling, cannot perform at these speeds. An alternative is to operate the high-speed motor within the UHV chamber. One can still obtain a good vacuum, see, for example, Ref. 12, as long as proper materials are used for lubrication and electrical insulation, and the motor heat is efficiently dissipated while in operation. We use a Köllmorgen brand (model RBE-00512-B11) vacuum rated brushless dc motor. It might also be possible to implement the velocity selector using an external motor with a ferrofluidic sealed feedthrough, although a shaft extending far enough for the dual blade assembly would likely still require support on lubricated bearing sleeves located within the chamber.

TABLE I. Specifications of the velocity selector design.

Description	Value
Sample-source separation (d)	200 mm
Sample diameter	8 mm
Source diameter	7 mm
Blade separation (L)	100 mm
Slot width (l_s)	13 mm
Tooth width (l_s)	37 mm
Pitch angle (ϕ)	0.35 rad

Design of the photon blocking velocity selector involves numerous compromises to allow room for sample transfer, translation of a microbalance flux monitor into the atom beam, differential pumping around the oven assembly, etc. The analysis of the previous section was important for guiding the design process at this point, and we eventually arrived at the geometry specified in Table I. Drawings of the assembly are given in Fig. 2, including a cut away showing the spring loaded upper cartridge bearing. Not shown is the

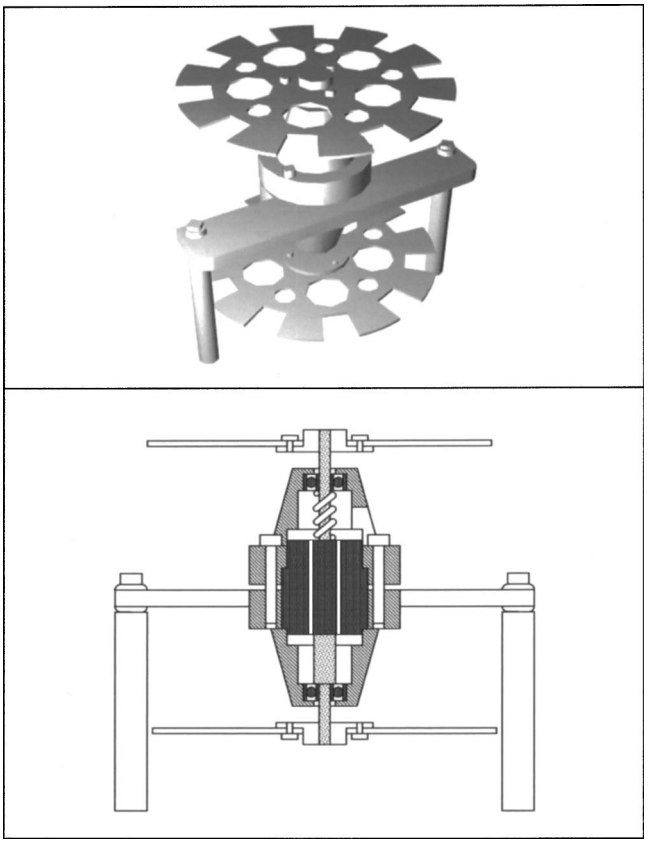

FIG. 2. Schematic of prototype velocity selector construction: (a) Three-dimensional view, and (b) cut-away view showing the bearing support. Not shown is the water-cooled aluminum block clamped to the assembly.

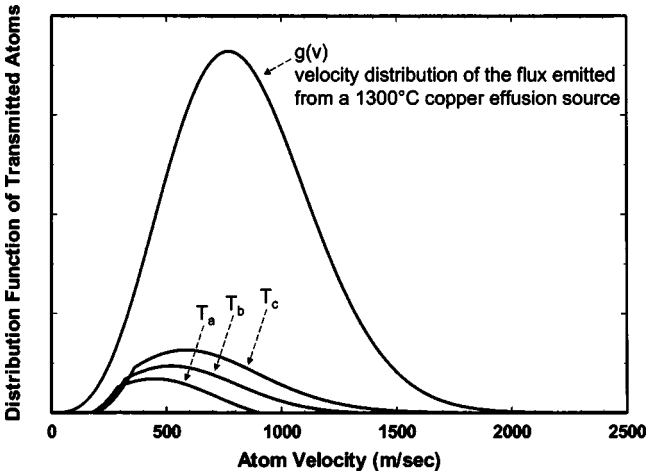

FIG. 3. The velocity distribution of the flux transmitted along paths *a*, *b*, and *c* of Fig. 1, calculated using the velocity selector parameters. Shown on the same scale is the flux incident on the velocity selector from the 1300 °C copper atom source.

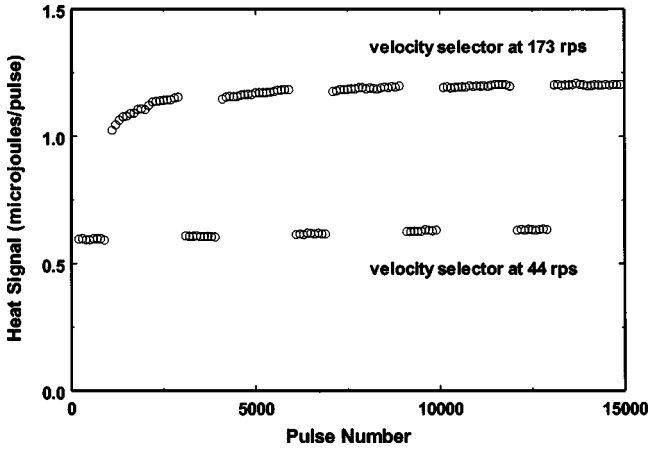

FIG. 4. The heat signal measured from the 1300 °C copper oven. Each data point is the independent average of 100 pulses. Each pulse has 40 ms duration and delivers 2.0×10^{12} atoms/cm^2 at the sample when the velocity selector is turning at high speed (173 revolutions per second). No atoms are transmitted when it is turning at low speed (44 revolutions per second).

water-cooled aluminum block which clamps around the assembly. The angle subtended by the circular sample at the source is 2.3°, which is small enough that $\cos(\theta)\approx1$ for any trajectory. However, it still requires that the chopper tooth widths are much larger than the slot widths, in order to block all photon trajectories (including 2 mm extra overlap used here for alignment tolerance). The blades shown in Fig. 2 were an early prototype where each had a duty factor close to 50%.

The velocity selector is operated with an upper speed limit of 173 Hz, which for a 1300 °C copper atom source gives the theoretical transmission curves shown in Fig. 3. The curve labelled $g(v)$ is the velocity distribution of the atoms without the photon block in place. The curves labelled T_a, T_b, and T_c are the velocity distributions with the photon block in place, calculated as the product $g(v)\cdot B'$ for the three different trajectories of Fig. 1. In this case, *a* and *c* are the most extreme trajectories subtended by the sample, having angles of ±2.3° from the source normal, while *b* is a nondivergent trajectory. The total atom flux transmitted to the sample is 9% of that without the photon block.

IV. CALORIMETRY OPERATION

For our experiments, we use an additional chopper to break the atom into pulses of 40 ms duration and 4 Hz repetition rate, in order to best match the thermal and electrical time constants of the calorimetric heat detector. Each of these 40 ms pulses is chopped into ~167 velocity-selected pulses which are summed together over the detector time constants. Figure 4 shows the calorimeter signal for copper deposition on polyimide, recorded with the velocity selector turning at high speed for a calculated atom transmission of 9%, and also at a lower speed where the atom transmission is 0%. The signal recorded in the latter case is due to scattered light which illuminates the entire chamber when the additional slow chopper, which is near the glowing oven, opens. This radiation signal is about 1% that measured without the velocity selector in place, and could be attenuated further with better optical baffling between the oven compartment and the rest of the chamber, or by repositioning the slow chopper so that it does not modulate the scattered light as strongly. However the radiation background shown is easily measured and subtracted from the calorimetry signal, and provides us with useful data regarding the metallization process. For instance, a sharp increase in the optical absorbance at higher copper coverages indicates the percolation of adsorbed metal clusters into a continuous metal film on the polyimide substrate, which allows an estimation of the number density of the clusters.

More general than its application as a photon block, the velocity selector is a variable transmission *atom* block. It can be used to stop all of the atoms during the recording of background measurements, or to attenuate the deposition flux to any degree desired, and it works with a much faster response time than can be achieved by ramping the oven temperature. As discussed in the next section, however, there are some significant effects of the velocity selector on the properties of the transmitted beam that need to be taken into account.

V. PROPERTIES OF THE TRANSMITTED BEAM

Since the faster atoms are more likely to be blocked, the average kinetic energy of the transmitted beam is lower than that of the original effusion flux. This has a direct effect on reaction calorimetry measurements, since the kinetic energy of atoms from the hot source adds to the reaction heat signal during equilibration with the room-temperature substrate. And in some cases, the reaction cross sections might depend on the energy of the incident atoms. From the velocity weighted flux distribution of Eq. (3), the average kinetic energy of the beam without the velocity selector is given by 2RT, which for the 1300 °C copper atom source equals 26 kJ/mol. From the velocity distribution of the transmitted beam given by Eq. (4), we calculate that the average kinetic energy with the velocity selector in place is 14 kJ/mol. Both

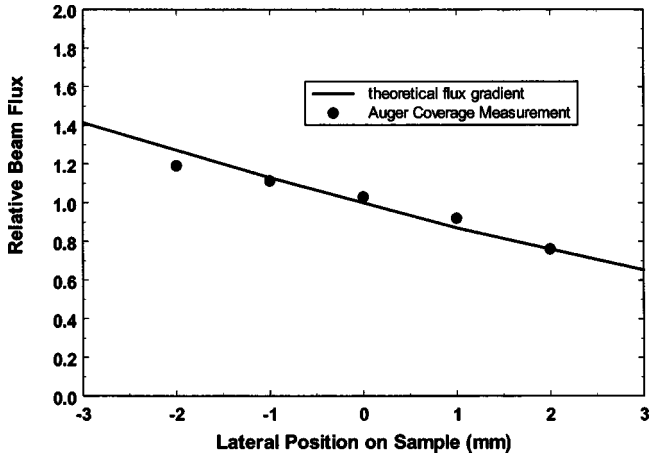

FIG. 5. Calculated flux profile across the center of the Cu beam, in the direction of chopper blade motion (x axis). Also shown, scaled to fit, is the thickness profile of the copper film deposited on an Au/mica substrate, as determined using Auger spectroscopy.

of these energies are significantly less than the chemical energy generated by copper atom condensation to form the bulk metal,[9] a value of 337 kJ/mol.

Another consequence of the velocity selector, which is made apparent by consideration of Fig. 3, is that the angular dependence of the transmission function results in a nonuniform deposition across the sample. Referring to Fig. 1, more of the high-velocity atoms will pass successfully along trajectory c than those launched along trajectories a or b, because the slot opening on the second blade intersects that trajectory sooner. As a result, the side of the sample toward which such trajectories are angled will see a higher flux. Figure 5 shows the flux gradient across the beam along the x axis, calculated using Eq. (4) for the 1300 °C copper source and assuming equilibrium effusion. Also shown are our Auger measurements of the film thickness at different positions along the x axis for deposition of the copper on a clean flat Au/mica substrate.

The thickness gradient could be ameliorated by placing the source and sample further apart, or by giving them narrower apertures. However, this would be at the cost of a lower total flux, and also is not as necessary as might first appear. The experimental signal is an average of that created at different local coverages on the sample, but this average will be weighted by the flux at each position, which narrows the distribution. More significantly, because the sample is circular, the leading and trailing edges of the sample where the flux is most extreme have less surface area, and so contribute less to the heat signal.

As a test, we consider two model cases where the reaction heat is coverage dependent, and calculate the total heat generated per pulse as a function of average coverage across the surface. Figure 6(a) is an example where the differential heat varies as an exponential function of the local coverage. We show the signal which would be created by the nonuniform velocity selected beam described by Eq. (4), and also by a uniform beam with the same number of atoms per pulse. It can be seen that in this case there is little effect on even a quantitative analysis of the calorimetric data.[7] Similarly, Fig.

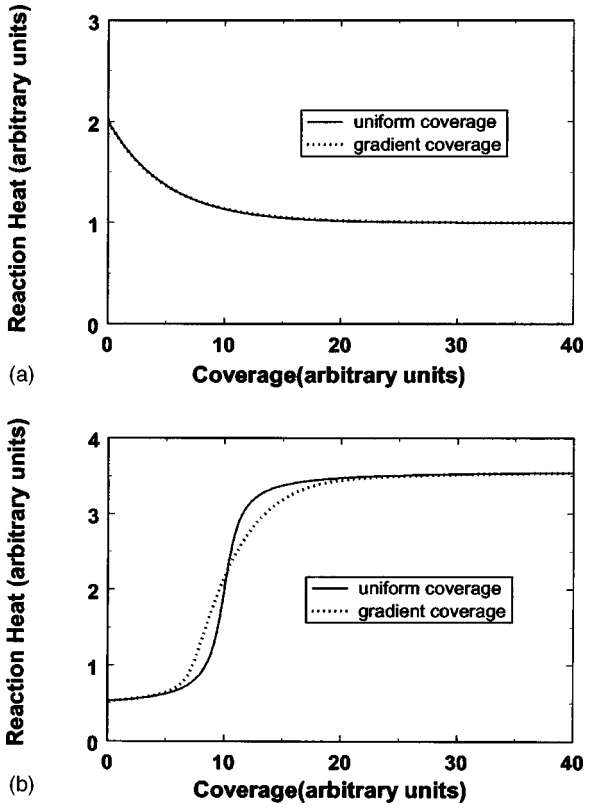

FIG. 6. The reaction heat generated per pulse as a function of the average deposited coverage. (a) and (b) use two different model functions for the reaction heat as a function of local coverage. In each figure, the heat is shown both for the case of a uniform deposition and for the case where the deposition gradient is as shown in Fig. 5.

6(b) is for a model case where the local reaction heat increases almost as a step function with coverage. In this case, there is certainly some loss of coverage resolution due to the nonuniform flux created by the velocity selector, but the data still allow for qualitative analysis.[7]

We do find a further issue associated with the flux gradient, that it appears to affect the accuracy of quartz crystal microbalance measurements of the beam flux. Even in the case of a uniform flux, commercial microbalances do generally require calibration measurements.[13] In our experiments, we can determine the number of atoms per pulse by calibrating our thermal sensor using laser heating pulses, and then comparing the measured heat of atom deposition in thick films to the tabulated standard enthaply of the formation of the metal atoms. In the case of calcium atom deposition, where the oven temperature is low, we can accurately measure the deposition heat without the velocity selector in place, and then the microbalance and calorimeter measurements of the beam flux are in reasonable agreement. However, when the velocity selector is in place, we find that the microbalance measurement overestimates the flux by an amount which varies widely between experiments, but is usually on the order of 100%. For an experiment in which the absolute flux through the velocity selector was checked by film thickness measurements using Auger spectroscopy, the microbalance overestimated the flux by 85%.

The response of a quartz crystal microbalance to nonuniform loading is typically discussed in terms of a variation in

sensitivity across the crystal,[14,15] the usual planar design being more sensitive in the center and less so around the edges, though with significant asymmetry. While this would make the response more sensitive to the exact position and orientation of the microbalance in the beam, it does not explain why a thickness gradient across the crystal would always lead to a higher apparent mass. This effect may instead be explained by a study[16] which shows that nonuniform mass loading of a microbalance crystal can lead to a localization of the mechanical resonance in the region where it is most heavily loaded. This would be consistent with our observations here, and also in Ref. 3 where flame emission spectroscopy was used to calibrate a microbalance with a flat-topped circular deposition partially covering the crystal.

VI. NONIDEAL EFFUSION

The foregoing analysis has been for a supposed equilibrium effusion source. In fact, the source is a crucible with an orifice diameter of 7 mm and an orifice length of ~35 mm (depending on the metal fill), while the equilibrium vapor pressure of copper at 1300 °C would be 2×10^{-2} Torr with a corresponding atom MFP of ~2.5 mm. We will not attempt a quantitative analysis of the resultant flux distribution, as there must be significant but unknown temperature gradients along the length of the crucible and from the crucible to the oven thermocouple. Speaking qualitatively, the flux will be somewhat more forward directed than for an effusive cosine distribution. However the length/diameter ratio of the crucible is small enough that the flux at 2.3° off normal should still be ~90% of the on-line flux, calculated in the limit where the MFP is larger than the diameter.[1] And since the MFP here is smaller than the crucible diameter, the effective channel length is diminished, providing even less forward channeling.

An additional nonideality is that the emitted flux at high temperatures will be less than that predicted assuming molecular flow, eventually increasing only as the square root of the equilibrium vapor pressure. Under these conditions, the velocity distribution of the emission is most depleted in slow atoms, which means also that the velocity selector will appear more opaque to the beam. Using the analysis provided by Pauly[1] to estimate the velocity distribution in the case where the MFP is just less than the orifice diameter, we calculate that the transmission probability through the velocity selector would decrease about 20%. However since the MFP in our experiments is actually substantially less than the orifice diameter, the oven flux will be also be depleted in fast atoms, and so the transparency of the velocity selector may be closer to that calculated for the ideal source. We cannot directly test the transmission because the oven flux at a given temperature changes substantially upon cooling the oven, opening the chamber to install the velocity selector, and then reheating. The absolute value of the transmitted flux which we measure is in reasonable agreement with that calculated for an ideal source. Also, the flux gradient measured across the transmitted beam agrees well with that calculated assuming an ideal effusive source. This suggests that nonideal effects are not too significant here.

ACKNOWLEDGMENTS

The authors thank Professor Charles Campbell for discussion regarding the velocity selector, and Y. K. Sohn for assistance with the Auger spectroscopy. The authors gratefully acknowledge funding provided by NSERC Canada. One of the authors (R. J. M.) thanks NSERC for a PGS fellowship.

[1] H. Pauly, in *Atomic and Molecular Beam Methods*, edited by G. Scoles (Oxford University Press, Oxford, UK, 1988), Vol. 1, Chap. 4.
[2] M. A. Herman and H. Siter, *Molecular Beam Epitaxy* (Springer, Berlin, 1989), Chap. 2.
[3] J. T. Stuckless, N. A. Frei, and C. T. Campbell, Rev. Sci. Instrum. **69**, 2427 (1998).
[4] J. T. Stuckless, D. E. Starr, D. J. Bald, and C. T. Campbell, Phys. Rev. B **56**, 13496 (1997).
[5] D. E. Starr, J. H. Ranney, J. H. Larsen, J. E. Musgrove, and C. T. Campbell, Phys. Rev. Lett. **87**, 106102 (2001).
[6] C. T. Campbell and D. E. Starr, J. Am. Chem. Soc. **124**, 9212 (2002).
[7] R. Murdey and J. T. Stuckless, J. Am. Chem. Soc. **125**, 3995 (2003).
[8] S. S. Hon, J. Richter, and J. T. Stuckless, Chem. Phys. Lett. **385**, 92 (2004).
[9] *CRC Handbook of Chemistry and Physics*, edited by D. R. Lidde, 75th ed. (CRC Press, Boca Raton, Fla, 1991).
[10] C. J. N. van den Meijdenberg, in *Atomic and Molecular Beam Methods*, edited by G. Scoles (Oxford University Press, Oxford, UK, 1988), Vol. 1, Chap. 13.
[11] G. Comsa and R. David, Surf. Sci. Rep. **5**, 145 (1985).
[12] J. Libuda, I. Meusel, J. Hartmann, and H.-J. Freund, Rev. Sci. Instrum. **71**, 4395 (2000).
[13] C. J. Barnes and J. P. Reilly, Surf. Sci. **463**, L613 (2000).
[14] R. M. Mueller and W. White, Rev. Sci. Instrum. **39**, 291 (1968).
[15] P. J. Cumpson and M. P. Seah, Meas. Sci. Technol. **1**, 544 (1990).
[16] R. Oltra and I. O. Efimov, Rev. Sci. Instrum. **66**, 1136 (1995).